Eur. Phys. J. AP **3**, 253–262 (1998)

THE EUROPEAN PHYSICAL JOURNAL APPLIED PHYSICS

New voltage strategy of a AC/DC two-cascaded converter with near unity power factor

S. Pierfederici, B. Davat[a], and M. Abignoli[b]

Groupe de Recherche en Électrotechnique et Électronique de Nancy, 2 avenue de la forêt de Haye, 54516 Vandœuvre-les-Nancy Cedex, France

Received: 19 February 1998 /Revised: 24 June 1998 / Accepted: 26 June 1998

Abstract. A new control method of cascaded power supply converters using the sliding approach is presented here. Variable Structure Control enables the problems of stability brought about by cascaded converters to be solved and its robust behaviour acts against variations in the load parameters and supply voltage.

PACS. 84.30.Jc Power electronics; power supply circuits – 84.70.+p High-current and high-voltage technology: power systems; power transmission lines and cables

1 Introduction

Various applications of the theory of variable structured systems to power electronic converters already exist in literature. They mainly focus on one input systems: switch control [1,2]. For a two-cascaded converter, several switches could be independently controlled and one must consider this theory in the case of multiple input systems [3].

For a one phase power supply, switching power supplies can be considered. Their control should ensure accurate regulation of the output voltage even though there is a unity power factor. To obtain this, the use of a cascade with Boost and Forward converters seems to be a solution. This choice presents several advantages, robustness thanks to the intrinsic properties of the Forward converter, galvanic insulation and the possibility of working in continuous conduction mode for the Boost stage.

Nevertheless, controlling a two-converter cascade is a difficult issue. In fact, from the Boost stage, the Forward converter acts as a negative resistor. An increase in its input voltage involves a decrease in its input current, and *vice-versa*. This problem already seen with the input filter design in the switching power supplies [4,5] could be solved thanks to linear regulators (method of the average equivalent scheme [6]). Consequently the design uses small-signal modelling. This paper presents an alternative method based on the theory of variable structured systems using large-signal modelling. This theory implies using the sliding mode control which will be reconsidered before studying the system modelling in question. For a given application, the control parameters and their principles will be set out in detail before presenting various experimental results.

2 Sliding mode control

The principle of control consists in leading the system state trajectory to a constraint, called the switching surface. To do this, an adaptive switching logic makes the trajectory converge to the surface before maintaining it with oscillations in various places. We are then in the neighbourhood of the stable stationary point of the system. The ideal sliding trajectory is obtained when the system trajectory slides on the switching surface and corresponds to a logic where frequency control is unlimited. Among the various properties of sliding mode control, some are well adapted to controlling the power electronic converter [7,8]:

- the trajectory of the system state variable belongs to a manifold, the dimension of which is lower than the dimension of the state space. So the order of the differential equations which rules the functioning of the system, is reduced;
- in some conditions, the sliding mode technique is robust to parameter variations;
- the sliding mode technique is a mathematical method used to analyse a discontinuous system. It is specially adapted to systems with discontinuous control or with systems formed by two subsystems switching from one to another and transferring power *via* the discontinuous process.

One can briefly recall the principle of the method. If one considers the following non-linear analytical system

[a] e-mail: davat@ensem.u-nancy.fr

[b] Michel Abignoli died in March 1997.

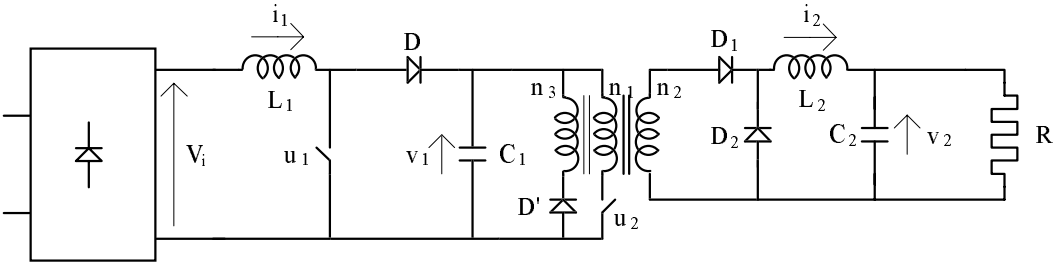

Fig. 1. Boost - Forward converter used.

where f is an analytical function:

$$\dot{\mathbf{x}} = f(\mathbf{x},\, t,\, u) \tag{1}$$

where $\mathbf{x}$ the state vector belongs to X, an open sphere of $\Re^n$ and u is the function control belonging to $\Re^m$. For an m-dimensional surface, if s is a continuous function s: $X \to \Re^m$, the following set S:

$$S = \{\mathbf{x} \in \Re^n / s(\mathbf{x}) = 0\} \tag{2}$$

defines a manifold of X, the dimension of which is $(n-m)$. This is called sliding manifold or sliding surface.

The law of variable structured control is obtained by giving the control variable one of 2^m possible state drawbacks which always aims to bring back the state trajectory to the surface. If the state trajectory reaches the surface and the movement is forced to proceed here (or at least to stay in the neighbourhood of the surface), the sliding motion exists on S and every time it is in the neighbourhood of S, we can verify the following assertion:

$$\frac{d}{dt}\left(s(\mathbf{x})^t \cdot s(\mathbf{x})\right) < 0. \tag{3}$$

The stability study needs the preliminary calculation of the equivalent control of the system [7]. It allows the differential equation corresponding to the ideal sliding motion to be obtained with precision. This trajectory corresponds to the intersection of the m switching surfaces defined by the the m S-component functions noted s_i. If we suppose that the sliding mode exists on the manifold $s(\mathbf{x}) = 0$, matrix $\mathbf{G}$ can be defined as:

$$\mathbf{G}_{i,j} = \frac{\partial s_i}{\partial \mathbf{x}_j} \tag{4}$$

and one looks for the equivalent continuous control u_{eq} which maintains the state trajectory on the surface. One must solve the equation:

$$\dot{s} = \mathbf{G} \cdot f(\mathbf{x},\, t,\, u_{eq}) + \frac{\partial}{\partial t} s = 0 \tag{5}$$

It is clear that if a time t_0 such as $s\big(\mathbf{x}(t_0)\big) = 0$ exists, then (3) imposes movement of the system on the manifold $s(\mathbf{x}) = 0$. In the particular case where (1) is written under the form:

$$\dot{\mathbf{x}} = f(\mathbf{x},\, t) + \mathbf{B}(\mathbf{x},\, t) \cdot u,\; f \in \Re^n,\; \mathbf{B} \in \Re^{n \times m} \tag{6}$$

then (5) becomes:

$$\dot{s} = \mathbf{G} \cdot f(\mathbf{x},\, t) + \mathbf{G} \cdot \mathbf{B}(\mathbf{x},\, t) \cdot u_{eq} + \frac{\partial}{\partial t} s = 0 \tag{7}$$

and the equivalent control is easily obtained:

$$u_{eq} = -\left(\mathbf{G} \cdot \mathbf{B}(\mathbf{x},\, t)\right)^{-1} \cdot \left(\mathbf{G} \cdot f(\mathbf{x},\, t) + \frac{\partial}{\partial t} s\right) \tag{8}$$

One can now express the dynamic of the system on the sliding surface and deduce the poles of the close loop for a given operating point:

$$\begin{cases} \dot{\mathbf{x}} = f(\mathbf{x},\, t) - \mathbf{B}(\mathbf{x},\, t) \cdot \left(\mathbf{G} \cdot \mathbf{B}(\mathbf{x},\, t)\right)^{-1} \\ \qquad\qquad \times \left(\mathbf{G} \cdot f(\mathbf{x},\, t) + \dfrac{\partial}{\partial t} s\right). \\ s(\mathbf{x}) = 0 \end{cases} \tag{9}$$

3 System modelling

The studied two-cascaded converter is shown in Figure 1. It is formed with a one stage Boost loaded by a Forward converter. This second converter has been built so that the dimensioning factor is maximum ($n_3 = n_1 = \frac{n_2}{2}$ [6]). Each switch is formed with a one power electronic component and a non-resistive switching circuit. The duty cycle is limited to 0.5 to avoid transformer saturation. Moreover the converter is supposed to work in continuous conduction mode.

The state equation of the system can be expressed in the following form:

$$\dot{\mathbf{X}} = \mathbf{A} \cdot \mathbf{X} + \mathbf{B}(\mathbf{X}) \cdot \mathbf{U} + \mathbf{C} \cdot \mathbf{V}_i \tag{10}$$

where the vector $\mathbf{X}$ is formed by the currents i_1 and i_2 flowing into the inductors L_1 and L_2, the voltages V_1 and V_2 across the capacitors C_1 and C_2 and the flux flowing through the transformer supplied winding:

$$\mathbf{X} = [i_1 \;\; v_1 \;\; \phi \;\; i_2 \;\; v_2]^t. \tag{11}$$

The vector u represents the control of the two switches:

$$\mathbf{U} = \begin{bmatrix} u_1 \\ u_2 \end{bmatrix} \tag{12}$$

where the variables u_1 and u_2 are equal to 1 or 0 depending on the state of conduction of the switches.

$$\mathbf{E}=\begin{bmatrix} 0 & -\frac{1}{L_1} & 0 & 0 & 0 & 0 & \frac{1}{L_1} & 0 \\ \frac{1}{C_1} & 0 & \frac{\Re}{n_3\cdot C_1} & 0 & 0 & 0 & 0 & 0 \\ 0 & -\frac{1}{n_3} & 0 & 0 & 0 & 0 & 0 & 0 \\ -\frac{K_p}{C_1} & -K_i & -\frac{K_p\cdot\Re}{n_3\cdot C_1} & 0 & 0 & 0 & 0 & K_i \\ 0 & 0 & 0 & 0 & 0 & 1 & 0 & 0 \\ 0 & 0 & 0 & 0 & -\frac{1}{L_2\cdot C_2} & -\frac{1}{R\cdot C_2} & 0 & 0 \\ 0 & 0 & 0 & 0 & 0 & 0 & 0 & 0 \\ 0 & 0 & 0 & 0 & 0 & 0 & 0 & 0 \end{bmatrix} \quad \mathbf{F}=\begin{bmatrix} \frac{v_1}{L_1} & 0 \\ -\frac{i_1}{C_1} & K \\ 0 & \left(\frac{1}{n_1}+\frac{1}{n_3}\right)\cdot v_1 \\ \frac{K_p\cdot i_1}{C_1} & -K\cdot K_p \\ 0 & 0 \\ 0 & \frac{n_2}{n_1}\cdot\frac{v_1}{L_2\cdot C_2} \\ 0 & 0 \\ 0 & 0 \end{bmatrix} \tag{15}$$

$$\text{where } \mathbf{K}=-\frac{\Re\cdot\phi}{C_1}\cdot-\frac{n_2}{n_1}\cdot\left(\frac{v_2}{R\cdot C_1}+\frac{C_2}{C_1}\cdot\frac{d}{dt}v_2\right) \tag{16}$$

Matrices **A**, **B** and **C** have the form:

$$\mathbf{A}=\begin{bmatrix} 0 & -\frac{1}{L_1} & 0 & 0 & 0 \\ \frac{1}{C_1} & 0 & \frac{\Re}{C_1\cdot n_3} & 0 & 0 \\ 0 & -\frac{1}{n_3} & 0 & 0 & 0 \\ 0 & 0 & 0 & 0 & -\frac{1}{L_2} \\ 0 & 0 & 0 & \frac{1}{C_2} & -\frac{1}{R\cdot C_2} \end{bmatrix}$$

$$\mathbf{B}=\begin{bmatrix} \frac{V_1}{L_1} & 0 \\ -\frac{i_1}{C_1} & -\frac{n_2}{n_1}\cdot\frac{i_2}{C_1}-\frac{\Re\cdot\phi}{C_1}\cdot\left(\frac{1}{n_1}+\frac{1}{n_3}\right) \\ 0 & V_1\cdot\left(\frac{1}{n_1}+\frac{1}{n_3}\right) \\ 0 & \frac{n_2}{n_1}\cdot\frac{V_1}{L_2} \\ 0 & 0 \end{bmatrix}$$

$$\mathbf{C}=\begin{bmatrix} \frac{1}{L_1} \\ 0 \\ 0 \\ 0 \\ 0 \end{bmatrix} \tag{13}$$

A change of variable leads us to consider the term $\frac{i_2}{C_2}-\frac{v_2}{R\cdot C_2}$ as the new state variable, which represents the variation of voltage across C_2, rather than the current i_2 in the inductor L_2. We will show later that this choice allows the control robustness of the output stage.

The appropriate control mode must ensure a unity power factor for the converter being used. Thus the shape of the current flow into the inductor L_1 should be sinusoidal over a half-period of the power supply in phase with the supply voltage. This is realized with a PI controller (with constants K_i and K_p) which is applied to voltage error V_1, thus delivering the reference i_{1ref} of the current flowing into the inductor L_1. Consequently the number of the system state variables are increased by one.

The introduction in the state vector of the rectifier output voltage V_i and the reference voltage allows to put the state equation into the form given by (6):

$$\dot{\mathbf{Y}}=\mathbf{E}\cdot\mathbf{Y}+\mathbf{F}(\mathbf{Y})\cdot\mathbf{U} \tag{14}$$

with:

$$\mathbf{Y}=[i_1\ \ v_1\ \ \phi\ \ i_{1ref}\ \ v_2\ \ \frac{d}{dt}v_2\ \ V_i\ \ v_{1ref}]^t.$$

See equations (15) and (16) above.

In this last equation, variables V_i and v_{1ref} are assumed to be constant. Taking into consideration their time variations implies adding other pseudo state variables which increase the size of the system. But this is not necessary because the part of the matrix **E** involving these variables owns poles which are independent of the control parameters.

4 Control method

4.1 Principle

The control method is presented in Figure 2. The system is considered as being two single input subsystems (the Boost and the Forward converters) with their own switching surfaces. This decentralizing switching technique allows better control of the variations of the different system variables and of the operating limit value (voltage V_1 lower than V_i, limitation of the current peaks involving the saturation of the different magnetic elements...). The block "filter" represents a first order filter which is used to generate a first order reference signal.

The two following switching surfaces are selected:

$$\begin{aligned} \mathbf{S}_1:&\ a_{11}\cdot\mathbf{Y}_1-a_{14}\cdot\mathbf{Y}_4+a_{12}\cdot(\mathbf{Y}_2-\mathbf{Y}_{2ref})+a_{15}\cdot\mathbf{Y}_5=0 \\ \mathbf{S}_1:&\ a_{25}\cdot(\mathbf{Y}_5-\mathbf{Y}_{5ref})+a_{26}\cdot\mathbf{Y}_6=0 \end{aligned} \tag{17}$$

The components appearing in these equations are those of vector **Y** defined by the relation (15), Y_{2ref} and Y_{5ref} are the reference voltage v_{1ref} and v_{2ref}, the coefficients a_{ij} are positive.

This choice of surfaces allows us to optimize the first stage control in accordance with the set of the key parameters and to obtain interesting robustness properties for the output. Each surface is formed by one term with fast variations proportional to a current error and an additional term with slow variations proportional to a voltage error. The terms with fast variations allow to avoid dangerous fluctuations of current in the converter. The coefficient a_{15} will prove that no interaction, between the control of the two stages, is necessary to obtain stability. The stability

$$\lambda^5 \cdot \left(\lambda + \frac{a_{25}}{a_{26}}\right) \cdot \left[\lambda^2 + \frac{Y_2 \cdot (a_{12} + a_{14} \cdot K_p) + Y_1 \cdot (a_{11} - a_{14} \cdot L_1 \cdot K_i)}{Y_2 \cdot a_{11} \cdot C_1 - Y_1 \cdot (a_{12} + a_{14} \cdot K_p) \cdot L_1} \cdot \lambda + \frac{Y_2 \cdot \left(a_{11} \cdot \Re + a_{14} \cdot n_3^2 \cdot K_i\right)}{n_3^2 \cdot (Y_2 \cdot a_{11} \cdot C_1 - Y_1 \cdot (a_{12} + a_{14} \cdot K_p) \cdot L_1)}\right] = 0. \quad (22)$$

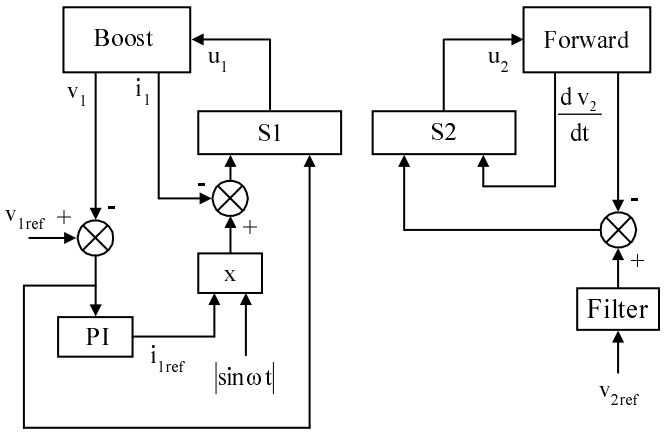

Fig. 2. Control scheme of the converter.

condition of each subsystem on its switching surface and the placing of the poles, will give the values of the different parameters used in the switching surface definition.

4.2 Calculation of the poles on the sliding surface

One supposes in this part that coefficients a_{ij} which define the switching surfaces are constant. Matrix $\mathbf{G}$ in (4) becomes:

$$G = \begin{bmatrix} a_{11} & a_{12} & 0 & 0 & -a_{14} & a_{15} & 0 & 0 & 0 \\ 0 & 0 & 0 & 0 & 0 & a_{25} & a_{26} & 0 & 0 \end{bmatrix} \quad (18)$$

The choice of non-zero coefficients in the matrix is closely linked to the functioning of the converter and the appropriate control properties. For each subsystem, we only consider the useful coefficients directly involved in the control. The voltage v_2 is an exception to this as it is taken into account for the switching surface S_1 which is associated to the Boost converter of the input stage.

The behaviour of the system in question should be studied by first calculating the equivalent control and by replacing u by u_{eq} in the differential equation controlling the system. Equation (8) can be rewritten as:

$$u_{eq} = -\left[\mathbf{G} \cdot \mathbf{F}\left(\mathbf{Y}\right)\right]^{-1} \cdot \mathbf{G} \cdot \mathbf{E} \cdot \mathbf{Y} \quad (19)$$

hence:

$$\begin{aligned} \dot{\mathbf{Y}} &= \left[\mathbf{E} - \mathbf{F}\left(\mathbf{Y}\right) \cdot \left[\mathbf{G} \cdot \mathbf{F}\left(\mathbf{Y}\right)\right]^{-1} \cdot \mathbf{G} \cdot \mathbf{E}\right] \cdot \mathbf{Y} \\ &= \mathbf{A}_{eq}\left(\mathbf{Y}\right) \cdot \mathbf{Y}. \end{aligned} \quad (20)$$

This calculation of the equivalent control supposes that the matrix $\mathbf{G} \cdot \mathbf{F}$ can be inverted. Hence the condition:

$$\begin{aligned} a_{11} \cdot \frac{Y_2}{L_1} - (a_{12} + a_{14} \cdot K_p) \cdot \frac{Y_1}{C_1} &\neq 0 \\ a_{26} &\neq 0 \end{aligned} \quad (21)$$

The poles on the sliding surface are given by the roots of the characteristic polynomial associated to matrix A_{eq}. This leads to:

see equation (22) above.

This last result illustrates the order reduction of the system, resulting from the use of the two sliding surfaces S_1 and S_2 (two additional zero poles).

A stable system on the surface can be obtained when the real part of the poles are negative. This leads to the relations:

$$\begin{aligned} \frac{Y_2 \cdot (a_{12} + a_{14} \cdot K_p) + Y_1 \cdot (a_{11} - a_{14} \cdot L_1 \cdot K_i)}{Y_2 \cdot a_{11} \cdot C_1 - Y_1 \cdot (a_{12} + a_{14} \cdot K_p) \cdot L_1} &> 0 \\ \frac{Y_2 \cdot \left(a_{11} \cdot \Re + a_{14} \cdot n_3^2 \cdot K_i\right)}{n_3^2 \cdot (Y_2 \cdot a_{11} \cdot C_1 - Y_1 \cdot (a_{12} + a_{14} \cdot K_p) \cdot L_1)} &> 0 \end{aligned} \quad (23)$$

The coefficient a_{15} is not used in the procedure of placing the poles. So we choose $a_{15} = 0$.

4.3 Stability in the neighbourhood of S_2

The stability condition (3) in the neighbourhood of the switching surface S_2 can be expressed by the two following inequalities:

$$\begin{aligned} \lim_{\substack{S_2(Y) \to 0^+ \\ u_2 = u_2^+}} \left(\frac{\partial S_2}{\partial Y} \cdot \frac{\partial Y}{\partial t} + \frac{\partial S_2}{\partial t}\right) &< 0 \\ \lim_{\substack{S_2(Y) \to 0^- \\ u_2 = u_2^-}} \left(\frac{\partial S_2}{\partial Y} \cdot \frac{\partial Y}{\partial t} + \frac{\partial S_2}{\partial t}\right) &> 0. \end{aligned} \quad (24)$$

The surface S_2 has to control the Forward output voltage. For the switch of this converter, the natural control consists in switching it off when the trajectory is above the surface, or by switching it on. This gives:

$$\begin{aligned} u_2^+ &= 0 \\ u_2^- &= 1 \end{aligned} \quad (25)$$

With regard to the reference variations, especially when starting up the system, equality (7) allows us to transform the previous inequalities into:

$$a_{25} \cdot Y_6 - a_{26} \cdot \left(\frac{Y_5}{L_2 \cdot C_2} + \frac{Y_6}{R \cdot C_2}\right) - a_{25} \cdot \frac{\partial\, Y_{5ref}}{\partial\, t} < 0$$

$$\begin{aligned} a_{25} \cdot Y_6 - a_{26} \cdot \left(\frac{Y_5}{L_2 \cdot C_2} + \frac{Y_6}{R \cdot C_2} - \frac{\frac{n_2}{n_1} \cdot Y_2}{L_2 \cdot C_2}\right) \\ - a_{25} \cdot \frac{\partial\, Y_{5ref}}{\partial\, t} > 0. \end{aligned} \quad (26)$$

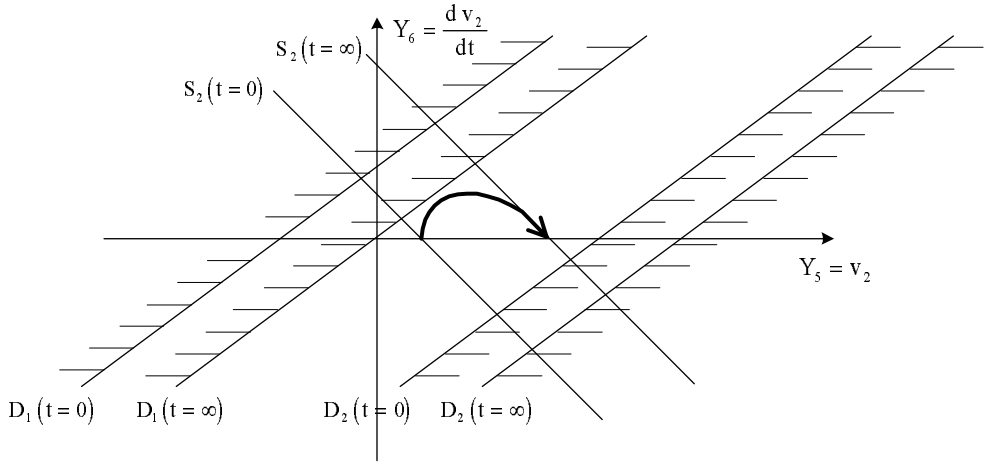

Fig. 3. Evolution of state variables Y_5 and Y_6 in the phase plane, with $\frac{a_{26}}{a_{25}} < R \cdot C_2$.

These relations show that in the case of rough variations of voltage reference Y_{5ref} (for a step load variation for example), the second inequality is not feasible. Also, a stable domain does not exist in the neighbourhood of S_2. So the system which can never reach the surface is unstable.

If we now suppose that $\dfrac{\partial Y_{5ref}}{\partial t}$ is bounded every time, it is possible to display the domain of stability graphically. Indeed, if we suppose that the input voltage Y_2 is constant, the previous relations define in the plane $Y_2 = \text{cte}$, a domain limited by two lines D_1 and D_2:

$$D_1 : \left(1 - \frac{a_{26}}{a_{25}} \cdot \frac{1}{R \cdot C_2}\right) \times Y_6 - \frac{a_{26}}{a_{25}} \cdot \frac{Y_5}{L_2 \cdot C_2} - \frac{\partial Y_{5ref}}{\partial t} = 0$$

$$D_2 : \left(1 - \frac{a_{26}}{a_{25}} \cdot \frac{1}{R \cdot C_2}\right) \cdot Y_6 - \frac{a_{26}}{a_{25}} \cdot \frac{Y_5}{L_2 \cdot C_2} + \frac{a_{26}}{a_{25}} \cdot \frac{\frac{n_2}{n_1} \cdot Y_2}{L_2 \cdot C_2} - \frac{\partial Y_{5ref}}{\partial t} = 0. \quad (27)$$

Two cases must be considered:

- $\dfrac{a_{26}}{a_{25}} < R \cdot C_2$ (Fig. 3)
We notice that the system can continuously move in a stable domain when, at the initial time, the initial point belongs to this domain and the line D_2 is to the right of the point of origin. This results in the condition:

$$(Y_5)_0 < m \cdot Y_2 - \frac{a_{25}}{a_{26}} \cdot L_2 \cdot C_2 \left(\frac{\partial Y_{5ref}}{\partial t}\right)_{max} \quad (28)$$

where m is the transformer ratio n_2/n_1.
From this last result, we can deduce that when the regulated output voltage reaches the limit value $m \cdot Y_2$, the variations of the reference must get slower and slower until they reach zero for the value $m \cdot Y_2$. This result is independent of the load. The relationship (28) must be considered in the most critical case which corresponds to the minimal allowable value of Y_2 (in fact the maximal value of the supply voltage).

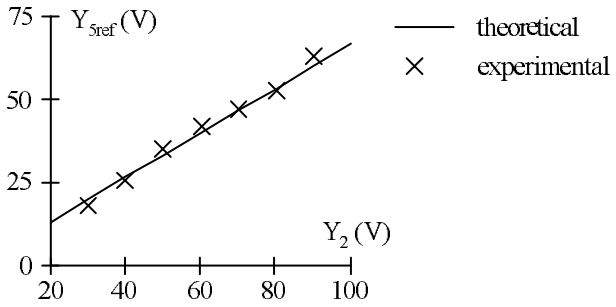

Fig. 5. Limit values of the voltage references.

- $\dfrac{a_{26}}{a_{25}} > R \cdot C_2$
Only the shape of the domain changes (Fig. 4), the observations made previously are the same. The maximum rate of variation of the reference, in moving from one stationary point to another, is given by (28). It is possible to check this last result against experimental tests by looking for the allowable maximum reference values for given speeds of variation and supply voltage when we choose the origin as initial point and a reference signal which verifies the following equation:

$$Y_{5ref}(t) = (Y_{5ref})_{max} \cdot \left(1 - \mathrm{e}^{-\frac{t}{\tau}}\right) \Rightarrow \left(\frac{\partial Y_{5ref}}{\partial t}\right)_{max} = \frac{(Y_{5ref})_{max}}{\tau} \quad (29)$$

Condition (28) can be rewritten as:

$$(Y_{5ref})_{max} < \frac{m \cdot Y_2 \cdot \tau}{\frac{a_{25}}{a_{26}} \cdot L_2 \cdot C_2} \cdot \quad (30)$$

In this test, the ratio a_{25}/a_{26} is set to 10^4, the time constant is equal to 0.01 s and m is equal to 2.

The measures have been realized with a regulated switching power supply. For practical reasons it was im-

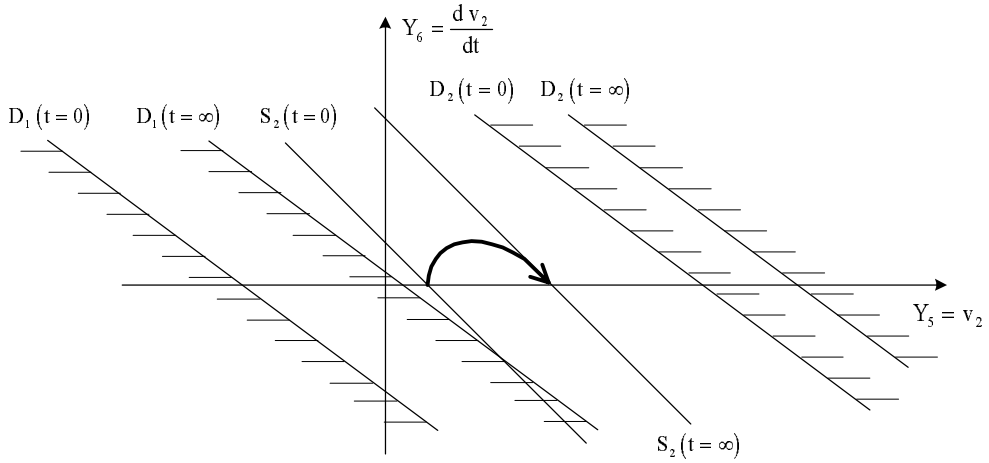

Fig. 4. Evolution of the state variables Y_5 and Y_6 in the phase plane, with $\frac{a_{26}}{a_{25}} > R \cdot C_2$.

possible to pursue the test with voltage values of Y_2 that were too high, because destructive instability had begun. The experimental results are shown in detail in Figure 5 and justify the theoretical expression previously established.

Thus, this kind of control applied to a buck or Forward converter adapts perfectly to power supplies at low levels of output voltage where the dynamic of the system can be very fast. Nevertheless precautions must be taken with regard to the rate of variation of the reference at high levels of output voltage. But in each case, the output voltage, like the stability criteria, is independent of load variations.

5 Stability in the neighbourhood of S_1

Looking for a domain of stability around S_1 is difficult on account of the large number of variables which take part in this control. One can, nevertheless, suppose that the trajectory of the output system (the Forward variables) always moves on the switching surface S_2.

As previously, the stability domain is given by the two inequalities:

$$\lim_{\substack{S_1(Y)\to 0^+ \\ u_1=u_1^+}} \left(\frac{\partial S_1}{\partial Y}\cdot\frac{\partial Y}{\partial t}+\frac{\partial S_1}{\partial t}\right) < 0$$
$$\lim_{\substack{S_1(Y)\to 0^- \\ u_1=u_1^-}} \left(\frac{\partial S_1}{\partial Y}\cdot\frac{\partial Y}{\partial t}+\frac{\partial S_1}{\partial t}\right) > 0. \quad (31)$$

Control is the same as for the Forward system. We have $u_1^+ = 0$ for the Boost subsystem and $u_1^- = 1$, (31) becomes:

$$a_{11}\cdot\left(\frac{V_i - Y_2}{L_1}\right) + a_{12}\cdot\left(\frac{Y_1}{C_1}+\frac{\Re\cdot\phi}{C_1\cdot n_3}+K\cdot u_2\right)$$
$$-a_{14}\cdot\left(-\frac{k_p\cdot Y_1}{C_1}-k_i\cdot(Y_2-Y_{2ref})-\frac{k_p\cdot\Re\cdot\phi}{C_1\cdot n_3}-k_p\cdot K\cdot u_2\right) < 0$$

$$a_{11}\cdot\left(\frac{V_i}{L_1}\right) + a_{12}\cdot\left(\frac{\Re\cdot\phi}{C_1\cdot n_3}+K\cdot u_2\right)$$
$$-a_{14}\cdot\left(-k_i\cdot(Y_2-Y_{2ref})-\frac{k_p\cdot\Re\cdot\phi}{C_1\cdot n_3}-k_p\cdot K\cdot u_2\right) > 0 \quad (32)$$

Because one supposes that S_2 is the locus of a sliding motion, one can replace the control u_2 by u_{2eq}. This approximation is similar to averaging, over one high frequency period of the Forward switch, all the system state parameters. It is then possible to suppress in the equations all the terms involving the magnetising current (its average value being zero seen from the capacitor C_1). Hence:

$$K = -\frac{m\cdot Y_5}{R\cdot C_1}$$
$$u_{2eq} = \frac{Y_5}{m\cdot Y_2} \quad (33)$$

(32) may be rewritten as:

$$a_{11}\cdot\left(\frac{V_i - Y_2}{L_1}\right) + a_{12}\cdot\left(\frac{Y_1}{C_1}+\frac{Y_5^2}{R\cdot C_1\cdot Y_2}\right)$$
$$-a_{14}\cdot\left(-\frac{k_p\cdot Y_1}{C_1}-k_i\cdot(Y_2-Y_{2ref})+\frac{kp\cdot Y_5^2}{R\cdot C_1\cdot Y_2}\right) < 0$$

$$a_{11}\cdot\left(\frac{V_i}{L_1}\right) + a_{12}\cdot\left(-\frac{Y_5^2}{R\cdot C_1\cdot Y_2}\right)$$
$$-a_{14}\cdot\left(-k_i\cdot(Y_2-Y_{2ref})+\frac{k_p\cdot Y_5^2}{R\cdot C_1\cdot Y_2}\right) > 0. \quad (34)$$

From the second inequality, one deduces:

see equation (35) next page.

$$Y_2 > \frac{1}{2\cdot a_{14}\cdot k_i}\left[-\left(\frac{a_{11}\cdot V_i}{L_1} - a_{14}\cdot k_i\cdot Y_{2ref}\right) + \sqrt{\left(\frac{a_{11}\cdot V_i}{L_1} - a_{14}\cdot k_i\cdot Y_{2ref}\right)^2 + 4\cdot a_{14}\cdot k_i\cdot(a_{12}+a_{14}\cdot k_p)\cdot\frac{Y_5^2}{R\cdot C_1}}\right] = Y_{2lim} \tag{35}$$

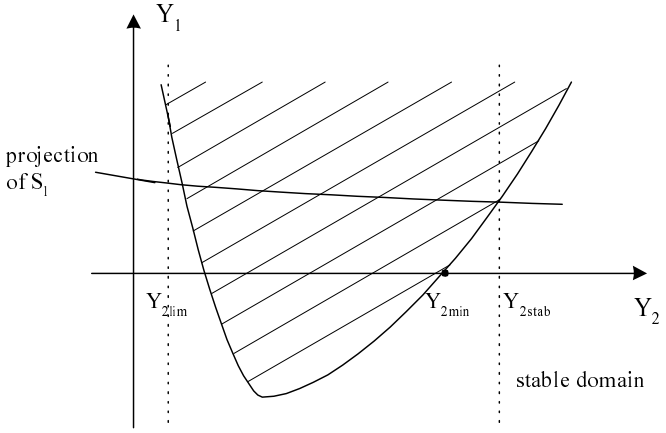

Fig. 6. Study of the stable sliding area of the surface S_1.

The first inequality can be interpreted graphically in the case where $a_{12}+a_{14}\cdot k_p$ is positive (Fig. 6). The other case is impossible because (23) is not verified for $Y_1 = 0$. The system is then unstable.

The trace left by the switching surface S_1, on the phase plane (Y_1, Y_2) when $a_{12}\cdot Y_{2ref}+a_{14}\cdot Y_4$ is maximum allows, us to determine the minimal value of Y_2, from which one obtains a stable domain. A numerical study shows that the nearer $a_{12}+a_{14}\cdot k_p$ is to zero, the nearer this value is to the supply voltage V_i, but the larger the harmonic content of the supply current is (when a_{12} is non zero, it adds to the input current a square signal in phase with the supply).

6 Case of sliding surfaces with variable coefficients

The process is unchanged. The parameters of matrix $\mathbf{G}$ previously defined are time dependent functions. In using the general results seen in the introduction, we find the equivalent control of the system:

$$u_{eq} = -\left(\mathbf{G}\cdot F(\mathbf{Y})\right)^{-1}\cdot\left(\mathbf{G}\cdot\mathbf{E}+\dot{\mathbf{G}}\right) \tag{36}$$

hence:

$$\dot{\mathbf{Y}} = \mathbf{A}_{eq}\cdot\mathbf{Y}$$

with:

$$\mathbf{A}_{eq} = \mathbf{E} - F(\mathbf{Y})\cdot\left(\mathbf{G}\cdot F(\mathbf{Y})\right)^{-1}\cdot\left(\mathbf{G}\cdot\mathbf{E}+\dot{\mathbf{G}}\right).$$

The unity power factor is obtained by constraining the input current to follow a sinusoidal reference. This condition implies that in this study the coefficient a_{14} is proportional to $|\sin\omega\cdot t|$ where ω is the power supply pulsation. The stability study on the sliding surface leads to the following result:

$$\begin{aligned}P(\lambda) = \lambda^4\cdot\Bigg(\lambda+\frac{a_{25}}{a_{26}}\Bigg)\cdot\Bigg(&\lambda^3+\lambda^2\\ &\times\left[\frac{Y_2\cdot(a_{12}+k_p\cdot a_{14})+Y_1\cdot(a_{11}-a_{14}\cdot L_1\cdot k_i)}{Y_2\cdot a_{11}\cdot C_1 - Y_1\cdot(a_{12}+k_p\cdot a_{14})\cdot L_1}\right]\\ &+\lambda\cdot\left[\frac{Y_2\cdot k_i\cdot a_{14}\cdot n_3^2 - a_{11}\cdot Y_2\cdot\Re}{n_3^2\Big(Y_2\cdot a_{11}\cdot C_1 - Y_1\cdot(a_{12}+k_p\cdot a_{14})\cdot L_1\Big)}\right.\\ &\left.+\dot{a_{14}}\cdot\left(\frac{-k_i\cdot Y_1\cdot L_1 + k_p\cdot Y_2\cdot a_{14}}{Y_2\cdot a_{11}\cdot C_1 - Y_1\cdot(a_{12}+k_p\cdot a_{14})\cdot L_1}\right)\right]\\ &+\dot{a_{14}}\cdot\frac{k_i\cdot Y_2}{Y_2\cdot a_{11}\cdot C_1 - Y_1\cdot(a_{12}+k_p\cdot a_{14})\cdot L_1}\Bigg)\end{aligned} \tag{37}$$

Because of the system dynamic on the switching surface S_1, it is possible to change all the physical parameters by their average values which are calculated over a half-period of the power supply. The analysis of (37) leads to result (22). As regards the stability domain, only the stability in the neighbourhood of the switching surface S_1 is modified. Thus, (34) can be rewritten as:

$$\begin{aligned}&a_{11}\cdot\left(\frac{V_i - Y_2}{L_1}\right) + a_{12}\cdot\left(\frac{Y_1}{C_1} - \frac{Y_5^2}{R\cdot C_1\cdot Y_2}\right)\\ &- a_{14}\cdot\left(-\frac{k_p\cdot Y_1}{C_1} - k_i\cdot(Y_2 - Y_{2ref}) + \frac{k_p\cdot Y_5^2}{R\cdot C_1\cdot Y_2}\right)\\ &- \dot{a_{14}}\cdot Y_4 < 0\end{aligned}$$

$$\begin{aligned}&a_{11}\cdot\left(\frac{V_i}{L_1}\right) + a_{12}\cdot\left(\frac{Y_5^2}{R\cdot C_1\cdot Y_2}\right)\\ &- a_{14}\cdot\left(-k_i\cdot(Y_2 - Y_{2ref}) + \frac{k_p\cdot Y_5^2}{R\cdot C_1\cdot Y_2}\right) - \dot{a_{14}}\cdot Y_4 > 0.\end{aligned} \tag{38}$$

The equivalent of (35) becomes:
(*see equation (39) next page*);
which must be verified for every $t\in[0,\,\pi]$.

As regards the second condition, it implies translating down towards Figure 6 graphically, and so increases the value Y_{2stab}.

7 Controller design

Coefficients a_{ij} are chosen to respect the following criteria:

$$Y_2 > \frac{1}{2 \cdot a_{14} \cdot k_i}\left[-\left(\frac{a_{11} \cdot V_i}{L_1} - a_{14} \cdot k_i \cdot Y_{2ref} - \dot{a}_{14} \cdot Y_4\right) + \sqrt{\left(\frac{a_{11} \cdot V_i}{L_1} - a_{14} \cdot k_i \cdot Y_{2ref} - \dot{a_{14}} \cdot Y_4\right)^2 + 4 \cdot a_{14} \cdot k_i \cdot (a_{12} + a_{14} \cdot k_p) \cdot \frac{Y_5^2}{R \cdot C_1}}\right] = Y_{2lim} \quad (39)$$

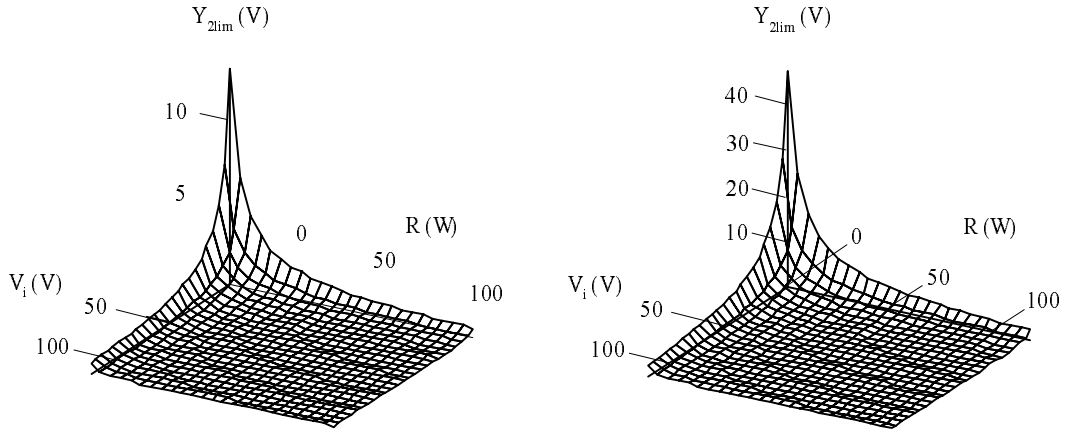

Fig. 7. Evolution of Y_{2lim} as a function of the load and the supply voltage ($Y_5 = 25$ V, left and $Y_5 = 50$ V, right).

– a unity power factor;
– accurate control of the output voltage;
– various stability conditions must be verified in the whole functioning domain.

Thus coefficients a_{ij} are set as follows:

$$\begin{aligned} a_{11} &= 1 & a_{15} &= 0 \\ a_{12} &= 5/1000 & a_{25} &= 1 \\ a_{14} &= |\sin(\omega t)| & a_{26} &= 10^{-4} \\ k_i &= 5 & n_1 &= 100 \\ k_p &= 15/100 & \Re &= 2.85 \times 10^6 \text{ H}^{-1} \end{aligned}$$

with $L_1 = L_2 = 3$ mH and $C_1 = 860$ μF $C_2 = 1000$ μF. The experimental operating point is defined by:

$$\begin{aligned} V_i &= 50 \sin(\omega t) \text{ V} \\ Y_{2ref} &= 100 \text{ V} \\ Y_{5ref} &= 25 \text{ V}. \end{aligned}$$

The graphical study of Y_{2lim} (Fig. 7), in the worst case (with R and v_{in} fixed, t and Y_4 are chosen to maximize (39) when Y_4 is physically limited by the application card), shows that (37) is always verified in the functioning domain. At the initial time, Y_2 (50v) is indeed greater than Y_{2lim}.

As regards the condition about Y_{2stab}, the graphical study in Figure 8 shows that the minimal value of Y_2 is almost independent of the load and is slightly greater than the supply voltage. The difference between the two values increasing with rising values of a_{12}. The coefficient a_{12} improves the stability but damages large signal stability criteria. The switching surface can be reached by simply starting the system at the zero crossing of the supply voltage. The value of Y_2 will be widely larger than the supply voltage.

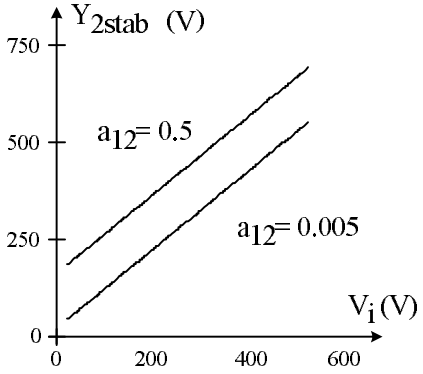

Fig. 8. Evolution of Y_{2stab} as a function of the load and the supply voltage.

The graph of condition (23) represented in Figure 9 as a function of the system operating point, shows that with the chosen parameters, the system is stable on the surface. For every operating point chosen, the real components of all the poles are negative. The system dynamic mainly depends on the parameter $a_{12} + K_p \cdot a_{14}$. The larger it is, the more the real components of the poles are negative. Nethertheless a significant increase of K_p or a_{12} could introduce significant current harmonics in the input current.

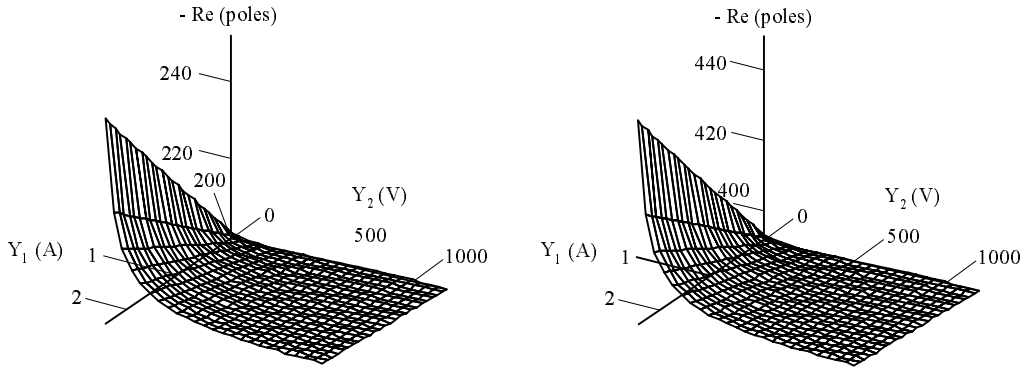

Fig. 9. Graph of the stability condition (23) ($K_p = 15/100$, left and $K_p = 30/100$, right).

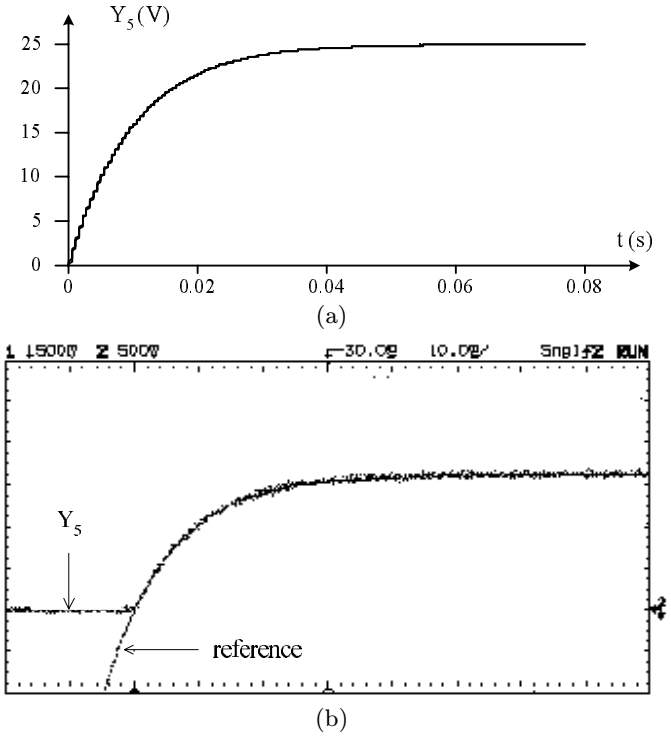

Fig. 10. Comparison between output and reference voltage. (a) Simulation; (b) experimental.

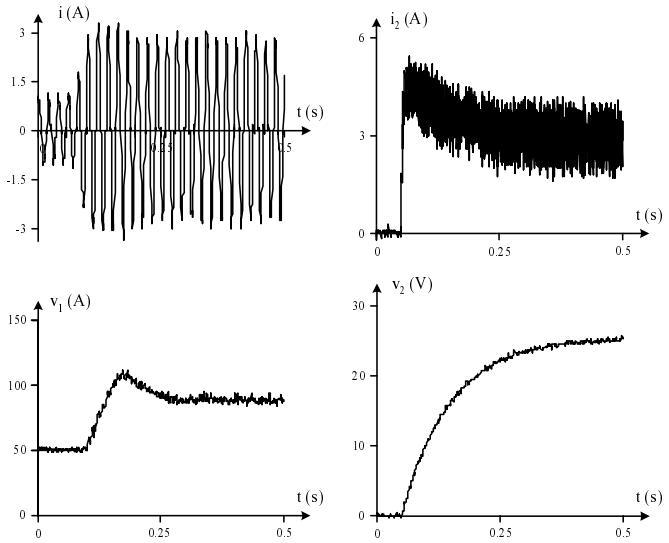

Fig. 11. Transient response of the various converter state variable.

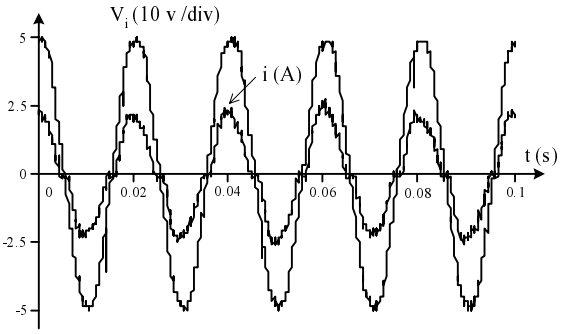

Fig. 12. Wave form of the supply current and the supply voltage of the converter.

8 Experimental results

For the experimental test, we use two hysteresis comparators to generate the two controls u_1 and u_2.

The main assumption in this study is that a sliding motion occurs on the switching S_2. This hypothesis is justified by the simulated and experimental results shown in Figure 10. The hypothesis made for the design of the parameters linked to the switching surface S_1 is correct.

The control starts when the power is on. The reference value Y_{2ref} is set to 90 V and the output voltage is set to 25 V with a resistive load R equal to 10 ohms. The transient state is shown in Figure 11. The results are consistent with the theory. The system is stable, the input current of the converter is near sinusoidal and the voltage Y_2 becomes stable in the neighbourhood of 90 V.

As seen on Figure 12, the supply current and the supply voltage are in phase. The lack of switching at the zero crossing of the power supply voltage is principally due to the relative little value the current which don't allow to change the output of the hysteresis controller. Thanks to

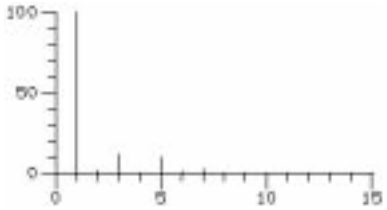

Fig. 13. Spectrum Analysis of the supply current.

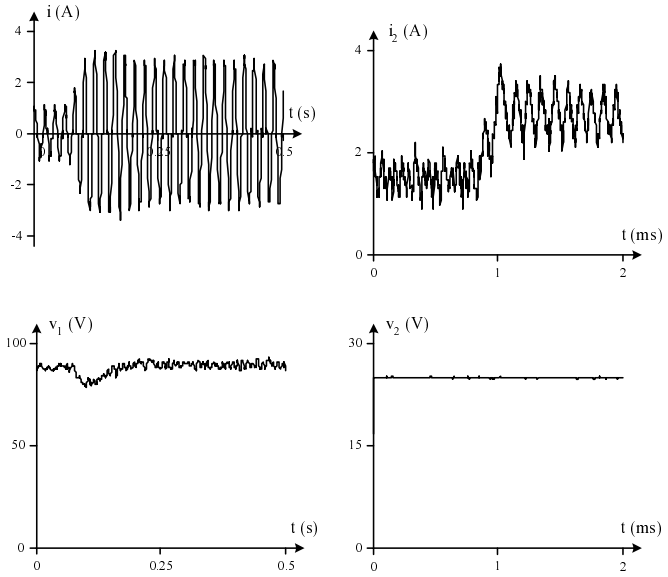

Fig. 14. Response of the various system state variables after a step load variation 20 Ω − 10 Ω.

a spectrum analysis of the input current (Fig. 13), we find that the THD is equal to 0.17 (which corresponds to a power factor equal to 0.986).

The system in steady state is submitted to a step load variation of 50% (load resistor goes from 20 to 10 ohms). The theory foresees a total robustness to this load variation. The results in Figure 14 seem to justify this assertion. We can easily observe the transient response of the Boost stage. The transient response of the Forward stage is realized in almost one cycle of commutation.

9 Conclusion

In this study, we have presented a new control strategy of a two-converter cascade. The proposed large-signal modelling allows the controller design to exist in a large functioning domain. A prototype has been built allowing us to confirm the theoretical approach. The new control strategy means that a sinusoidal absorption converter can be obtained, and this ensures accurate control of the output voltage (undulation rate less than 0.1%, robustness vis-à-vis variations in the load, as well as in the parameters and the supply voltage).

Nevertheless, precautions are required, especially for the rate of variation of the reference and the start of the control (necessity to start the system in a stable domain).

A study in the work of a 1 kW Boost-Forward converter based on the previous results and the close relationship between the equivalent control of sliding mode and the duty cycle of PWM technique, could allow the generations of robust unity power factor converters which combine the advantages of the PWM technique and the variable structured system technique.

References

1. L. Malesani, L. Rosseto, IEEE Trans. Power Electron. **10**, 302 (1995).
2. L. Rossetto, G. Spazzi, P. Tenti, B. Fabian, C. Licitra, IEEE Trans. Power Electron. **9**, 146 (1994).
3. A. Evan Groef, P.P.J van der Bosch, H.R Visser, EPE Firenze, **1**, 001 (1991).
4. F.C. Lee, Y. Yu, IEEE Trans. Aerospace Electron. Syst. **15** (1979).
5. P. Barrade, H. Piquet, Y. Cheron, J. Phys. III France, **6** 91 (1996).
6. F. Forest, J.P. Ferrieux, in *Alimentation à découpage Convertisseur à résonance* (Masson, collection technologies).
7. V. Utkin, I. Utkin , in *Sliding modes in control optimization* (Springer-Verlag, 1992).
8. W. Hahn, in *Theory and application of Liapunov's direct method* (Prentice-hall international, 1963).